Major category: Physical Sciences, Minor category: Atmospheric, and Planetary Sciences

Title: Intermediate-scale horizontal isoprene concentrations in the near-canopy forest

atmosphere and implications for emission heterogeneity

Carla E. Batista,<sup>1,2†</sup> Jianhuai Ye,<sup>3†\*</sup> Igor O. Ribeiro,<sup>1,2</sup> Patricia C. Guimarães,<sup>1,2</sup> Adan S. S. Medeiros,<sup>1,2,4</sup> Rafael G. Barbosa,<sup>2</sup> Rafael L. Oliveira,<sup>2</sup> Sergio Duvoisin Jr.,<sup>1,2</sup> Kolby J. Jardine,<sup>5</sup> Dasa Gu,<sup>6</sup> Alex B. Guenther,<sup>6</sup> Karena A. McKinney,<sup>7</sup> Leila D. Martins,<sup>8</sup> Rodrigo A. F. Souza,<sup>1,2\*</sup> Scot T. Martin.<sup>3,9\*</sup>

<sup>1</sup>Post-graduate Program in Climate and Environment, National Institute of Amazonian Research and Amazonas State University, Manaus, Amazonas, 69060-001, Brazil

<sup>2</sup>School of Technology, Amazonas State University, Manaus, Amazonas, 69065-020, Brazil

<sup>3</sup>School of Engineering and Applied Sciences, Harvard University, Cambridge, Massachusetts, 02138, USA

<sup>4</sup>Advanced Study Center at Tefé, Amazonas State University, Tefé, Amazonas, 69553-100, Brazil

<sup>5</sup>Climate and Ecosystem Sciences Division, Lawrence Berkeley National Laboratory, Berkeley, California, 94720, USA

<sup>6</sup>Department of Earth System Science, University of California, Irvine, California, 92697, USA

<sup>7</sup>Department of Chemistry, Colby College, Waterville, Maine, 04901, USA

<sup>8</sup>Department of Chemistry, Federal University of Technology-Paraná, Londrina, Paraná, 86047-125, Brazil

<sup>9</sup>Department of Earth and Planetary Sciences, Harvard University, Cambridge, Massachusetts, 02138, USA

Submitted March 2019 to Proceedings of the National Academy of Sciences of the United States of America

<sup>†</sup>These authors contributed equally to this study.

\*Correspondence to: Scot T. Martin (scot\_martin@harvard.edu), Rodrigo A. F. Souza (souzaraf@gmail.com), and Jianhuai Ye (jye@seas.harvard.edu)

### Abstract

1

2

3

4

5

6

7

8

9

10

11

12

13

14

15

16

17

The emissions, deposition, and chemistry of volatile organic compounds (VOCs) are thought to be influenced by underlying landscape heterogeneity at intermediate horizontal scales of several hundred meters across different forest sub-types within a tropical forest. Quantitative observations and scientific understanding at these scales, however, remain lacking, in large part due to a historical absence of canopy access and suitable observational approaches. Herein, horizontal heterogeneity in VOC concentrations in the near-canopy atmosphere was examined by sampling from an unmanned aerial vehicle (UAV) flown horizontally several hundred meters over the plateau and slope forests in central Amazonia during the morning and early afternoon periods of the wet season of 2018. Unlike terpene concentrations, the isoprene concentrations in the near-canopy atmosphere over the plateau forest were 60% greater than those over the slope forest. A gradient transport model constrained by the data suggests that isoprene emissions differed by 220% to 330% from these forest sub-types, which is in contrast to a 0% difference implemented in most present-day biosphere emissions models (i.e., homogeneous emissions). Quantifying VOC concentrations, emissions, and other processes at intermediate horizontal scales is essential for understanding the ecological and Earth system roles of VOCs and representing them in climate and air quality models.

- 18 Keywords: isoprene emissions, landscape heterogeneity, intermediate horizontal scales, Amazon
- 19 tropical forest, UAV measurements

# **Significance Statement**

Unquantified intermediate-scale heterogeneity in VOC emissions over Amazonia may be a key contributor to the observed discrepancy between measured and modeled VOC concentrations, but in situ measurements for investigating the possibility have been lacking. The measurements presented herein quantify horizontal VOC concentration gradients over different forest sub-types at the intermediate scale of several hundred meters. The results suggest that there are biases in both top-down estimates based on satellite or aircraft measurements, and bottom-up approaches based on leaf or tower measurements. The results demonstrate how observations collected by UAV-enabled technologies fill a missing niche among leaf-level, tower, aircraft, and satellite scales. Information at this previously unavailable scale is needed for accurate understanding and predictions related to changing forests under climate stress.

Volatile organic compounds (VOCs) emitted from forests have important roles in signaling among plants, animals, insects, and microbes, ecosystem functioning and health, and atmospheric chemistry and climate (1, 2). Tropical forests are the major global VOC source but are comparatively less studied and understood than their temperate and boreal counterparts (3). Tropical forest landscapes can have great heterogeneity and many forest sub-types at scales of 100's of meters (i.e., intermediate horizontal scales) (4, 5). In central Amazonia, rolling hills underlying the tropical forest north of the Amazon River give rise to plateaus interspersed by water-logged valleys, all dissected by streams and rivers and joined by sloped regions, at scales of hundreds of meters. Myriad forest sub-types and biodiversity result across this intermediate scale for reasons of water, sunlight, and soil, among other factors and variations (6, 7).

The landscape variability at intermediate scales is thought to be associated with variability in VOC emissions at the same scale (8). For any VOC, some tropical forest sub-types can have high emissions of that VOC whereas other sub-types can exhibit low emissions or pockets of net deposition, even as the forest as a whole emits in net. This emerging view of a heterogeneous patchwork of VOC emissions and deposition has important implications for interpreting results of earlier studies that have largely reported VOC observations from single locations, such as tower sites, with no information on the surrounding horizontal heterogeneity in VOC emissions and deposition. Atmospheric chemical transport models also do not accurately simulate VOC oxidation over tropical forests (9), and process-level models such as large-eddy simulations suggest that non-uniform VOC emissions from different forest sub-types can be one possible explanation (10-12). Measurements of VOC variability over the forest sub-types are needed to investigate this possibility as well as to improve predictive capabilities for models of emissions and reactive chemistry over these landscapes.

Topography is often a first surrogate of landscape variability and thus also of VOC emissions, especially in Amazonia (13, 14). Contributing factors tying topography to forest subtype are variations in elevation, slope, aspect, drainage, soil type, and microclimate, among others, that determine forest species composition and diversity. Flood-free plateau forest grows on the tops of rolling hills, and over 200 species are routinely identified in inventories (15). The soils are strongly leached, with low natural fertility and high acidity. By comparison, valley forests are populated by plants adapted to richer, waterlogged soils and wetlands. More than 100 species are typically identified in inventories (15). Slope forests have a mix of valley and plateau plant families. Estimates are on the order of 10,000 distinct tree species across Amazonia (5, 16). Herein, results are reported for investigating the heterogenity of isoprene concentrations in the near-canopy atmosphere over plateau, slope, and valley forest sub-types in the central Amazonian forest during the wet season of 2018. Isoprene is the non-methane VOC emitted in greatest quantities by land surfaces on Earth, as represented in the Model of Emissions of Gases and Aerosols from Nature (MEGAN) (3). One estimate is that isoprene emissions alone represent 70% of total VOCs emitted by plants globally into the atmosphere (17). Leading models such as MEGAN and others, however, are not presently able to predict emissions heterogeneity at the intermediate horizontal scales across forests, even as differences are thought to exist, in large part because of the absence of historical measurement platforms and data sets. For investigation of forest sub-types at intermediate scales without disturbance of the underlying landscape, chemical sampling and sensing by use of unmanned aerial vehicles (UAVs) represents an emerging frontier in atmospheric chemistry (18). In the present study, data sets of isoprene concentration were collected at intermediate scales by use of a UAV, and relative emission

54

55

56

57

58

59

60

61

62

63

64

65

66

67

68

69

70

71

72

73

74

75

differences were inferred by use of a gradient transport model constrained to the measured heterogeneity in concentrations over the different forest sub-types.

### **Results**

Different forest sub-types. The UAV collected samples for two different locations above the Adolfo Ducke Forest Reserve (hereafter, "Ducke Reserve") in central Amazonia across four weeks during the wet season from February 20 to March 15, 2018. The Ducke Reserve (10 km × 10 km) is located on the northern outskirts of Manaus, Brazil, in central Amazonia. Established in 1963, the reserve is recognized as a globally important site for the study of tropical forests (6, 14, 19). A tower ("MUSA" tower) is located within the Manaus Botanical Gardens (MUSA) of the reserve (Fig. 1) (see Materials and Methods). Valley and plateau regions in the tower vicinity are approximately 50 m and 120 m above sea level (asl), respectively, and they are joined by sloped regions.

Biodiversity in Ducke Reserve is well characterized by tree inventory surveys. The plant species and occurrence in the reserve have three major forest classifications, described as valley, slope, and plateau forest sub-types (13-15, 20). These forest sub-types are represented in gray, brown, and green in Fig. 1. Valley forest occurs along the sandy banks of streams. Flooding is frequent, and the sediment mixes with the forest litter. Canopy height varies from 20 to 35 m. Plateau forest grows in the highest areas in well-drained yet nutrient-poor clay soil. Canopy height ranges from 25 to 35 m. Emergent trees can reach 45 m. Slope forest dissects the landscape, bridging between the valley and plateau forests. It is characterized by clay soils in the higher reaches of the slopes and sandy-loam soils in the lower parts. Canopy height ranges from 25 to 35 m. Another important forest classification at Ducke Reserve, which is interspersed among these major topography-based classifications, is campinarana. It grows on extremely

nutrient-poor, poorly drained, white quartz sandy regions. Canopy height varies between 15 and 25 m.

99

100

101

102

103

104

105

106

107

108

109

110

111

112

113

114

115

116

117

118

119

120

121

Ribeiro et al. (20) presented information on the prevalent plant species in each of the forest sub-types at Ducke Reserve, as summarized in Table S1 (SI Appendix). The MUSA forestry staff inspected the actual plant species at locations A and B at the time of the UAV flights, and the species were identified as consistent with the inventory of Ribeiro et al. Some important families include Arecaceae (commonly referred to as palm trees), Caryocaraceae, Clusiaceae, Fabaceae (legumes), Lecythidaceae, Meliaceae, Mimosaceae (specialized legumes), Rapataceae, Solanaceae (nightshades), and Sapotaceae. The species that grow in abundance are distinct for each forest sub-type. The photographs shown in Fig. 2 of the slope and plateau forests at locations A and B highlight differences in forest composition at the two locations. **Concentrations in near-canopy atmosphere.** The UAV was launched and recovered from a platform atop the MUSA tower (3.003° S, 59.940° W; inset picture of Fig. 1) (see Materials and Methods). The longitude-latitude point of the MUSA tower is referred to as location A herein. The UAV flew 711 m to 2.997° S and 59.936° W. This longitude-latitude point is referred to as location B in the study. Locations A and B were located over plateau and slope forest sub-types, respectively. The UAV hovered over the canopy at location B and sampled VOCs. An automated sampler, mounted to the UAV, collected the VOC samples in cartridges (21). Simultaneous VOC sampling took place on the tower platform at location A. All samples were analyzed off-line by gas chromatography. For locations A and B, samples were collected cumulatively in 4 different cartridge tubes across a week for 20 min of sampling within each hour of 09:00-10:00, 10:10-11:10, 11:20-12:20, and 12:30-13:30 (local time; 4 h earlier relative to UTC). This approach captured daily trends while ensuring sufficient material for chemical analysis. Four composite

samples were collected each week for a total of four weeks over each location, resulting in a total of 32 samples.

Many compounds were identified in the collected samples, including isoprene,  $\alpha$ -pinene,  $\beta$ -pinene, nine other monoterpenes,  $\beta$ -caryophyllene, and three other sesquiterpenes, together representing a progressive set of  $C_5$ ,  $C_{10}$ , and  $C_{15}$  compounds (Fig. 1). After emitting into the atmosphere, these and other VOCs undergo atmospheric mixing and dilution as well as reactive chemical loss. An upward trend is common in the concentrations from morning to noon (3), which can be explained by increasing solar irradiance and temperature. Enzyme activity increases with temperature, and electron transport increases with sunlight until saturation, resulting in a tendency for increasing emissions of isoprene and many other terpenoid VOCs from plants and consequently for increasing near-canopy atmospheric concentrations, balanced against atmospheric dilution and chemical loss (22).

The isoprene concentrations were consistently higher over the plateau forest compared to over the slope forest. The mean weekly isoprene concentrations above the slope forest ranged from 1.0 to 3.3 ppb (Fig. 3a and SI Appendix, Table S2). The mean concentrations above the plateau forest ranged from 2.9 to 4.9 ppb. The mean weekly differences for isoprene concentration over the slope compared to over the plateau forest ranged from 1.5 to 2.7 ppb. For the overall data set, the mean isoprene concentration was 2.4 ppb over the slope forest, which can be compared to 4.4 ppb over the plateau forest, representing an increase of +80% for the latter. The calculated probability (*p*-value) for a two-way ANOVA analysis in location and time is < 0.001 for the null hypothesis that the two sets of isoprene concentrations were the same over locations A and B (SI Appendix, Table S3). An implication is that measurements from a single

tower placed at either location A or location B would have significant bias if taken as representative of the regional area of Ducke Reserve.

The observed isoprene concentrations can be compared to previous reports throughout Amazonia (SI Appendix, Section S1 and Table S4). The reported concentrations range from <1 ppb to 27 ppb, in part reflecting the heterogeneity of tropical forests. The mean observed concentrations of 2.4 ppb and 4.4 ppb for locations A and B thus lie within the literature range reported for Amazonia.

Unlike isoprene concentrations, the concentrations and time variability of  $\alpha$ -pinene, which is typically the monoterpene emitted in largest quantities by the forest, were similar over the plateau and slope forests (Fig. 3a). The *p*-value was 0.61 for the null hypothesis that the two sets of  $\alpha$ -pinene concentrations were the same over location A and location B (SI Appendix, Table S3). The ratio of the isopene concentration to the  $\alpha$ -pinene concentration is plotted in Fig. 3b. An advantage of this concentration ratio, compared to the isoprene concentration alone, is a mitigation of some possible confounding factors related to differences in transport and reactive loss to locations A and B compared to differences in emissions from forest sub-types at locations A and B. Across 09:00 to 13:30, the mean weekly ratios above the slope forest ranged from 11.4 to 23.7. The ratios above the plateau forest ranged from 27.1 to 42.1. These comparative ratios thus also suggest significantly higher emissions of isoprene by the plateau forest compared to by the slope forest given that the  $\alpha$ -pinene concentrations had similar values over the two forest sub-types.

### **Discussion**

Isoprene is emitted across the horizontal extent of the forest as myriad point emissions from the leaves of individual plants, and the isoprene concentration at the location of UAV

sampling in the atmosphere represents the sum of the contribution of each of these point emissions. After being released from a plant, the emitted isoprene is subject to convection in the vertical, advection in the horizontal, and atmospheric chemical reaction (loss) during transport to the location of sampling. Therefore, forest emissions that are directly underlying the point of UAV sampling, as well as forest emissions that are farther afield and delivered to the point of sampling by regional atmospheric transport, affect the isoprene concentration at the location of UAV sampling. Dispersion and reactive loss of isoprene occur between emission at the source region and arrival at the UAV receptor location. Taking these factors into account is required to relate the observed differences in isoprene concentrations at locations A and B to possible differences in the emissions of the underlying forest sub-types.

Herein, a two-dimensional gradient transport model is used to simulate isoprene concentrations over the atmospheric boundary layer (23, 24). Details of the model are described in Section S2 (SI Appendix). The model simplifies the lower part of the atmosphere as an incompressible fluid at constant pressure and takes into consideration longitudinal and vertical transport as well as possible in situ chemical reactions. To assess the extent to which the local forest sub-type influences the concentrations measured at the point of UAV sampling, upwind spatial zones of influence for the point of measurement were determined. The zones of influence are defined as the horizontal upwind distances  $x_1$ ,  $x_2$ ,  $x_3$ , and  $x_4$  that respectively contribute 0 to 25%, 25 to 50%, 50 to 75%, and 75 to 95% of the total concentration  $C^{\dagger}$  at the point of UAV sampling. More specifically, a small value of  $x_1$  corresponds to a significant influence by local emissions of the directly underlying and nearby surrounding forest on the atmospheric concentrations sampled by the UAV. Values of  $x_1$ ,  $x_2$ ,  $x_3$ , and  $x_4$  are obtained from the model (SI Appendix, Section S3 and Table S5). For the atmosphere of a tropical forest affected by urban

pollution, corresponding to the parameters of the reference case listed in Table S6 (SI Appendix), the intervals are 0 to 150 m ( $x_1$ ), 150 to 700 m ( $x_2$ ), 700 to 2350 m ( $x_3$ ), and 8300 m and beyond ( $x_4$ ). These values apply to both locations A and B because the meteorological conditions at both sites are similar. Sensitivity analyses were performed to evaluate the effects of the uncertainty in model parameters on the zones of influence, and  $x_1$  varies between 100 to 250 m across the sensitivity analysis compared to 150 m for the reference case (SI Appendix, Table S7).

The zones of influence of the reference case are further represented in Fig. 1 in translucent overlay on the forest sub-types surrounding locations A and B in the directional sector of the dominant winds (SI Appendix, Fig. S1). The plot shows that 25% of the total isoprene concentration  $C^{\dagger}$  at location A is modeled as strongly related to the emissions of the nearby plateau forest (i.e., lying within the first dashed line position at  $x_1$ ) and likewise at location B to the emissions of the nearby slope forest (see also SI Appendix, Fig. S2). For the next 25% of  $C^{\dagger}$ , represented by the second dashed line at  $x_2$ , there is an influence of all three forest sub-types, although the specific portions of the forest contributing emissions to locations A and B remain distinct. The next 50% of  $C^{\dagger}$  beyond the  $x_2$  line can be understood as contributed by a pattern of repeating forest sub-types, representing a non-distinct average across the regional forest. For comparison, a low-flying aircraft or fixed-wing UAV might have an averaging kernel comparable to this local regional average.

The effect of sampling height above the local canopy on the measured concentrations was considered. For the reference case, the ratio  $C^{\dagger}(15 \text{ m})$ : $C^{\dagger}(47 \text{ m})$  is modeled as 1.21. UAV sampling was also carried out in late 2017 at height differences of 40 to 50 m over the plateau forest nearby location A, and the average ratio was 1.22 (SI Appendix, Table S8). A similar value was observed by sampling at a 44-m height difference along an 80-m tall tower situated in

a plateau forest about 100 km away for the daily period of 09:00 to 15:00 (LT) during the wet season (25). The same study showed that the variability in isoprene concentrations at these altitudes over the plateau forest correlated strongly with the variability in emissions from the local forest. The implication of these results is that differences in sampling height over the local canopy height at location B (47 m) compared to location A (15 m) are not sufficient to explain the average ratio of 1.80 in isoprene concentrations, as observed herein. The observed increase of +80% can be partitioned approximately as +20% for differences in height and +60% for differences in emissions.

Inverse modeling was applied to the data set to determine the emissions difference necessary to sustain a concentration difference of +60% between locations A and B. For the reference case of the model, a difference between 220% to 330% in emissions between the plateau and slope forest sub-types is needed to sustain the observed concentration difference. The lower estimate of 220% is obtained by assuming that the emissions differences extend to the full range of  $x_1$  and  $x_2$  (700 m) from locations A and B whereas the upper estimate of 330% is obtained by assuming that the emissions differences are fully within the range of  $x_1$  (150 m). The magnitude in differences in emissions for the different forest sub-types can be rationalized by the different species compositions and environmental conditions, keeping in mind the heterogeneous ecosystem of the tropical forest and the estimate that 30% of trees in a tropical forest are estimated to emit isoprene (26).

Atmospheric Implications. Although processes at intermediate scales of several hundred meters across an ecosystem are believed to exert significant control over the magnitude and type of VOC emission and deposition, these processes remain incompletely understood qualitatively and less defined quantitatively. Emissions models for Amazonia in particular continue to have large

uncertainties, including the assignment of base emission capacities, meaning the emission expected for a set of standard environmental conditions. Emission capacities for various landscape types, in Amazonia and elsewhere, are largely estimated by two complementary methods (27). (1) In a mechanistic, bottom-up approach composition data of vegetation species for a landscape, instantaneous canopy conditions at a time of interest, and plant-level functional relationships for those conditions are combined to estimate landscape-scale emissions. (2) In an empirical, one-size-fits-all approach canopy-level gradient or eddy flux measurements obtained for a location within a landscape type are assumed to hold across the entire landscape.

236

237

238

239

240

241

242

243

244

245

246

247

248

249

250

251

252

253

254

255

256

257

258

Method 1 has worked well for temperate and boreal forests because of low species diversity, and under this condition enclosure measurements of VOC emissions of the known dominant plant types are possible. By comparison, method 1 has large uncertainties for tropical forests because immense biodiversity in species composition challenges an accurate inventory of vegetation species and emission variability among those species presents difficulties for accurate functional relationships. Available literature is small relative to the forest heterogeneity. Ideally, isoprene emission rates characteristic of each of these plant species apparent in Fig. 2 and listed in Table S1 (SI Appendix) would be known, and accurate bottom-up predictions of isoprene emissions over the different sub-forests could be possible. In reality, insufficient information is available and difficult to acquire, not just because of the large biodiversity but also because of the dependence of emissions from a single plant on environmental conditions. In this challenging context, UAV-based sample collection provides a new capability that effectively represents a local, landscape-average measurement-based integration kernel of emissions at intermediate scales across the myriad leaf-level and plant-level factors to provide qualitatively new kinds of data sets and quantify the differences in emissions of the different forest sub-types.

Method 2 has been successful for relatively homogeneous and open ecosystems characteristic of temperate and boreal regions, and vertical profiles from towers and tethered balloons have been successful in determining VOC fluxes and emissions within acceptable uncertainty. For tropical forests, however, method 2, representing a single-point approach, has large uncertainties because of a lack of suitable approaches for quantifying heterogeneity in fluxes over scales of a kilometer or less across the landscape (28). Even locally, tower locations may not be representative because a single tree next to a tower can bias the profile results, especially at lower sampling heights where the small footprint contains only a few trees. In Amazonia, most research towers have been located in locally elevated topographical regions (i.e., plateau forests; see also SI Appendix, Table S4), and previous emission estimates taken as representative of Amazonia can have bias based on the limits of available data sets.

Several of the shortcomings of methods 1 and 2 applied to tropical forests can be ameliorated, at least in part, by the complementary application of the newly emerging technology of UAV-based sampling approaches. The results presented herein demonstrate the possibility of UAV-based sampling to collect information efficiently at the intermediate scales across footprints centered at adjustable longitude-latitude coordinates, as needed for understanding the heterogeneity of tropical forests. Access of this type has potential for improved sampling over undisturbed forests as well as over forests in forbiddingly inhospitable landscapes, such as waterlogged or swampy regions. For example, as a practical matter, the VOC sampler on the UAV flew from location A to location B in 5 min for sampling over two different forest subtypes. As a general statement, near-canopy atmospheric measurements described in the literature of tropical forest have been largely confined to a small set of locations where there are towers (e.g., SI Appendix, Table S4), implying that spatial heterogeneity has been inadequately

captured. UAV systems can be fully operated by powerful onboard computer controllers coordinated with a satellite-based positioning system, all of which are standard on a commercial UAV such as that used in this study. Sampling with a UAV allows take-off and landing from the Earth's surface without the presence of a tower, thus eliminating an important constraint on the site locations for research. Moreover, a vertically stacked multi-UAV configuration as a type of floating tower is a further possibility. Limitations must also be borne in mind, however. Current commercially available UAVs have short flight times of < 1 h due to battery capacity and limited payload capacity (< 10 kg), and aerospace regulations can limit flight operations in real-world practice (18).

In summary, the presented results demonstrate intermediate-scale horizontal heterogeneity of VOC concentrations, specifically isoprene concentrations, in the near-canopy atmosphere over central Amazonia. Emission differences implied by the measurements are quantified as 220% to 330% for the different forest sub-types across this biodiverse landscape. For comparison, the state-of-the-art MEGAN model assumes homogeneity at this scale and provides 0% difference in emissions between the two forest sub-types. The explanation is that there has not been sufficient knowledge about horizontal heterogeneity to inform the MEGAN model. These findings call attention once more to re-addressing a longstanding scientific unknown related to forest heterogeneity, now in hand with newly emerging UAV-assisted technical possibilities to make progress on this unknown, for understanding and quantifying VOC emissions at intermediate scales to better understand the ecological and Earth system roles of VOCs and to better represent them in climate and air quality model simulations.

### **Materials and Methods**

303

304

305

306

307

308

309

310

311

312

313

314

315

316

317

318

319

320

321

322

323

324

325

Sampling Platforms. The hexacopter UAV (DJI Matrice 600) equipped with the VOC sampler was launched and recovered from a platform (3.5 m × 3.5 m) atop the MUSA tower in the Ducke Reserve. Details of the sampler are described in Section S4 (SI Appendix) and Ref. (21). The tower corresponded to location A of the study (3.0032° S, 59.9397° W; inset picture of Figure 1). Ground level was 120 m asl at location A. The tower had a height of 42 m, and local forest canopy height nearby the tower was 25 to 35 m. Location B (2.997° S, 59.936° W) was 711 m distant from the tower. Ground level was 85 m asl. Local canopy height at location B was also 25 to 35 m. **Sampling Strategy.** During a UAV flight, a sampling period for a single cartridge was 2.5 min. More specifically, as an example, two flights on one day between 09:00 and 10:00 corresponded to 5 min of sampling with one cartridge tube. In the same cartridge tube, samples were collected at the same period of the day (e.g., 09:00 to 10:00) for four days in a week to ensure sufficient material for chemical analysis, corresponding to 20 min or 3 L of sampling for this cartridge tube (SI Appendix, Table S2). This sampling strategy was taken to complement work on semivolatile organic compounds (SVOCs; 17.5 min sampling each flight; work not described herein). The strategy of sampling across a broader period also helped to average out otherwise possible confounding effects of sustained downdrafts or updrafts during a single sampling period. Samples were collected simultaneously over location A (with a handheld pump; GilAir PLUS, Gilian) for 15 m above local canopy and over location B (with VOC sampler) for 47 m above local canopy height. The lower ground level (asl) at location B required the sampling at a higher relative height above the canopy so that the UAV remained in the horizontal visual field of the flight operator positioned on the tower platform at location A. The influence of different

sampling heights was not significant enough, however, to account for observed concentration differences (see main text).

Chemical Analysis. Samples were anlyzed using thermal desorption gas chromatography coupled with a time-of-flight mass spectrometer (Markes BenchTOF-SeV) and a flame ionization detector (TD-GC-FID/TOFMS). Details of the analysis including TD-GC operation protocols, VOC detection limits, and uncertainties are provided in Section S5 (SI Appendix).

Acknowledgments. The Manaus Botanical Gardens (MUSA) of Ducke Reserve kindly provided access and logistical support. Funding. The Brazilian Federal Agency for Support and Evaluation of Graduate Education (CAPES) (88881.187481/2018-01), the Brazilian National Council for Scientific and Technological Development (CNPq), a Senior Visitor Research Grant of the Amazonas State Research Foundation (FAPEAM) (062.00568/2014 and 062.00491/2016), the Harvard Climate Change Solutions Fund, the Postdoctoral Program in Environmental Chemistry of the Dreyfus Foundation, and the Division of Atmospheric and Geospace Sciences of the USA National Science Foundation (AGS-1829025 and AGS-1829074) are acknowledged.

## References

- Holopainen JK (2004) Multiple functions of inducible plant volatiles. *Trends Plant Sci.* 9(11):529-533.
- 2. Laothawornkitkul J, Taylor JE, Paul ND, & Hewitt CN (2009) Biogenic Volatile Organic Compounds in the Earth System. *New Phytol.* 183:27-51.
- 3. Guenther AB, *et al.* (2012) The model of emissions of gases and aerosols from nature version 2.1 (MEGAN2.1): an extended and updated framework for modeling biogenic emissions. *Geosci. Model Dev.* 5(6):1471-1492.
- 4. Malhi Y, *et al.* (2002) An international network to monitor the structure, composition and dynamics of Amazonian forests (RAINFOR). *J. Veg. Sci.* 13(3):439-450.
- 5. ter Steege H, *et al.* (2013) Hyperdominance in the Amazonian tree flora. *Science* 342(6156):1243092.
- 6. Laurance WF, *et al.* (2004) Pervasive alteration of tree communities in undisturbed Amazonian forests. *Nature* 428(6979):171-175.

- 7. Myster RW ed (2017) Forest structure, function and dynamics in Western Amazonia (Wiley, New York), p 206.
- 8. Kaser L, et al. (2015) Chemistry-turbulence interactions and mesoscale variability influence the cleansing efficiency of the atmosphere. *Geophys. Res. Let.* 42(24):10,894-810,903.
- 9. Butler T, *et al.* (2008) Improved simulation of isoprene oxidation chemistry with the ECHAM5/MESSy chemistry-climate model: lessons from the GABRIEL airborne field campaign. *Atmos Chem Phys* 8(16):4529-4546.
- 10. Auger L & Legras B (2007) Chemical segregation by heterogeneous emissions. *Atmos Environ* 41(11):2303-2318.
- 11. Krol MC, Molemaker MJ, & de Arellano JVG (2000) Effects of turbulence and heterogeneous emissions on photochemically active species in the convective boundary layer. *Journal of Geophysical Research: Atmospheres* 105(D5):6871-6884.
- 12. Ouwersloot H, *et al.* (2011) On the segregation of chemical species in a clear boundary layer over heterogeneous land surfaces. *Atmos Chem Phys* 11(20):10681-10704.
- 13. Ribeiro JELdS, et al. (1999) Flora da Reserva Ducke : guia de identificação das plantas vasculares de uma floresta de terra-firme na Amazônia Central (INPA, Manaus) p 799.
- 14. Schietti J, *et al.* (2013) Vertical distance from drainage drives floristic composition changes in an Amazonian rainforest. *Plant Ecol. Divers.* 7(1-2):241-253.
- 15. Oliveira ANd, et al. (2008) Composição e diversidade florístico-estrutural de um hectare de floresta densa de terra firme na Amazônia Central, Amazonas, Brasil (Translation: Composition and floristic-structural diversity of one hectare of dense terra firme forest in Central Amazonia, Amazonas, Brazil). Acta Amaz. 38:627-641.

- 16. Cardoso D, *et al.* (2017) Amazon plant diversity revealed by a taxonomically verified species list. *Proc. Natl. Acad. Sci. U.S.A.* 114(40):10695-10700.
- 17. Sindelarova K, *et al.* (2014) Global data set of biogenic VOC emissions calculated by the MEGAN model over the last 30 years. *Atmos Chem Phys* 14(17):9317-9341.
- 18. Villa T, Gonzalez F, Miljievic B, Ristovski Z, & Morawska L (2016) An overview of small unmanned aerial vehicles for air quality measurements: present applications and future prospectives. *Sensors* 16(7):1072.
- 19. Oliveira ML, Baccaro F, Braga-Neto R, & Magnusson WE (2008) *Reserva Ducke: a biodiversidade Amazônica através de uma grade (Translation: Ducke Reserve: the Amazonian biodiversity through a grid)* (Áttema Design Editorial, Manaus) p 170.
- 20. Ribeiro JELS, Nelson BW, Silva MFd, Martins LSS, & Hopkins M (1994) Reserva florestal ducke: diversidade e composição da flora vascular. *Acta Amaz.* 24(1-2):19-30.
- 21. McKinney KA, *et al.* (2019) A sampler for atmospheric volatile organic compounds by copter unmanned aerial vehicles. *Atmos. Meas. Tech.* 12: 3123-3135.
- 22. Jardine KJ, *et al.* (2015) Green leaf volatile emissions during high temperature and drought stress in a central amazon rainforest. *Plants* 4(3):678-690.
- 23. Alfonsi G (2009) Reynolds-averaged navier–stokes equations for turbulence modeling. *Appl. Mech. Rev.* 62(4):040802.
- 24. Lenschow D (1995) Micrometeorological techniques for measuring biosphereatmosphere trace gas exchange. *Biogenic Trace Gases: Measuring Emissions from Soil* and Water:126-163.

- 25. Yáñez-Serrano AM, *et al.* (2015) Diel and seasonal changes of biogenic volatile organic compounds within and above an Amazonian rainforest. *Atmos. Chem. Phys.* 15(6):3359-3378.
- 26. Harley P, *et al.* (2004) Variation in potential for isoprene emissions among Neotropical forest sites. *Glob. Change Biol.* 10(5):630-650.
- Guenther A, et al. (2006) Estimates of global terrestrial isoprene emissions using
   MEGAN (Model of Emissions of Gases and Aerosols from Nature). Atmos. Chem. Phys.
   6(11):3181-3210.
- 28. Misztal PK, *et al.* (2016) Evaluation of regional isoprene emission factors and modeled fluxes in California. *Atmos. Chem. Phys.* 16(15):9611-9628.

# **Figure Legends**

- Fig. 1. Local topography surrounding the tower (location A) at the Manaus Botanical Gardens ("MUSA") of the Adolfo Ducke Forest Reserve in the central Amazon, Brazil. The UAV flight route from location A over the plateau forest to location B over the slope forest is shown by the red line. Zones of influence are shown in translucent overlay on the forest sub-types surrounding locations A and B (see also SI Appendix, Fig. S2). The sector angle of each translucent overlay represents the variability of wind direction in the steady trade winds during the period of study. The dashed arc lines within a sector represent transitions from one zone of influence  $x_i$  to the next.
- **Fig. 2.** Photographs of the trees of the plateau forest (location A, top panels) and the slope forest (location B, bottom panels) of Fig. 1. The downward images on the left of the top of the forest canopy were taken by a camera on the UAV. The upward images on the right from the ground through the canopy were taken by a hiker at those locations.
- Fig. 3. (a) Isoprene (orange) and α-pinene (green) concentrations and (b) isoprene-to-α-pinene concentration ratios. Panels A, B, C, and D represent weeks 1, 2, 3, and 4, respectively, of the measurement period. (square) Over the plateau forest for 15 m above local canopy height at location A of Fig. 1. (triangle) Over the slope forest for 47 m above local canopy height at location B of Fig. 1. The isoprene concentrations were consistently higher over the plateau forest compared to the slope forest. By comparison, no significant difference was observed for near-canopy α-pinene concentrations between the plateau forest and the slope forest. Data were collected and agregated in intervals of 09:00-10:00 (local time), 10:10-11:10, 11:20-12:20, and 12:30-13:30 of the morning hours. Local time was UTC minus 4 h.

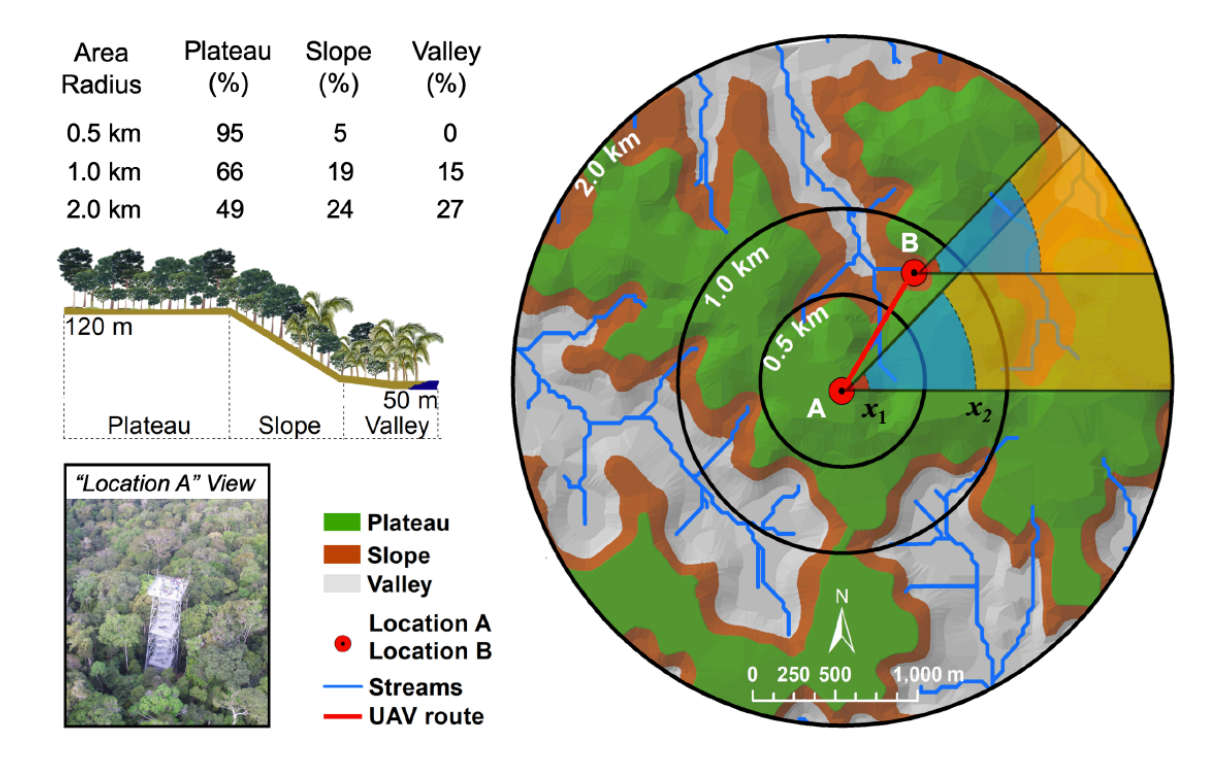


Figure 1

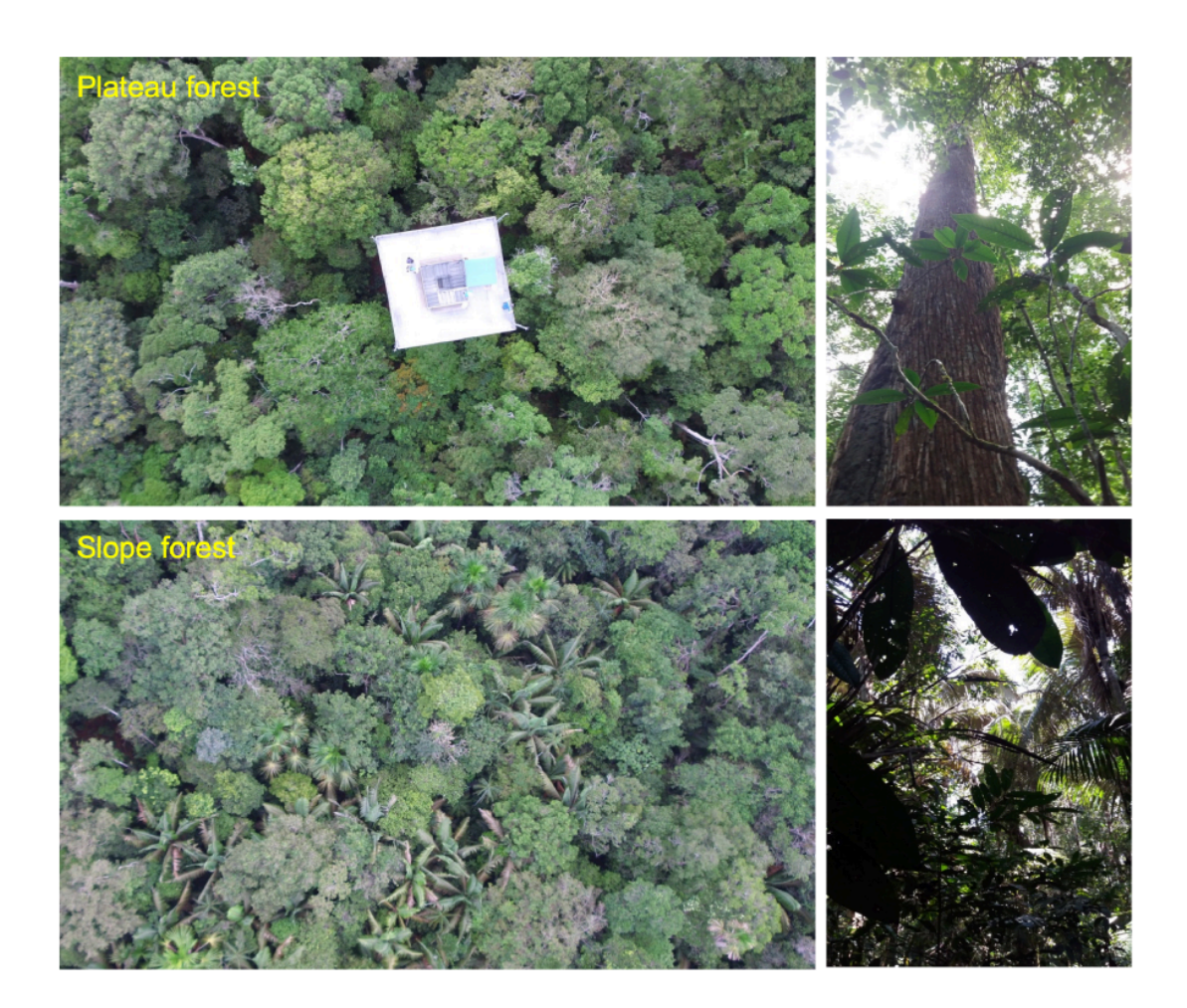


Figure 2

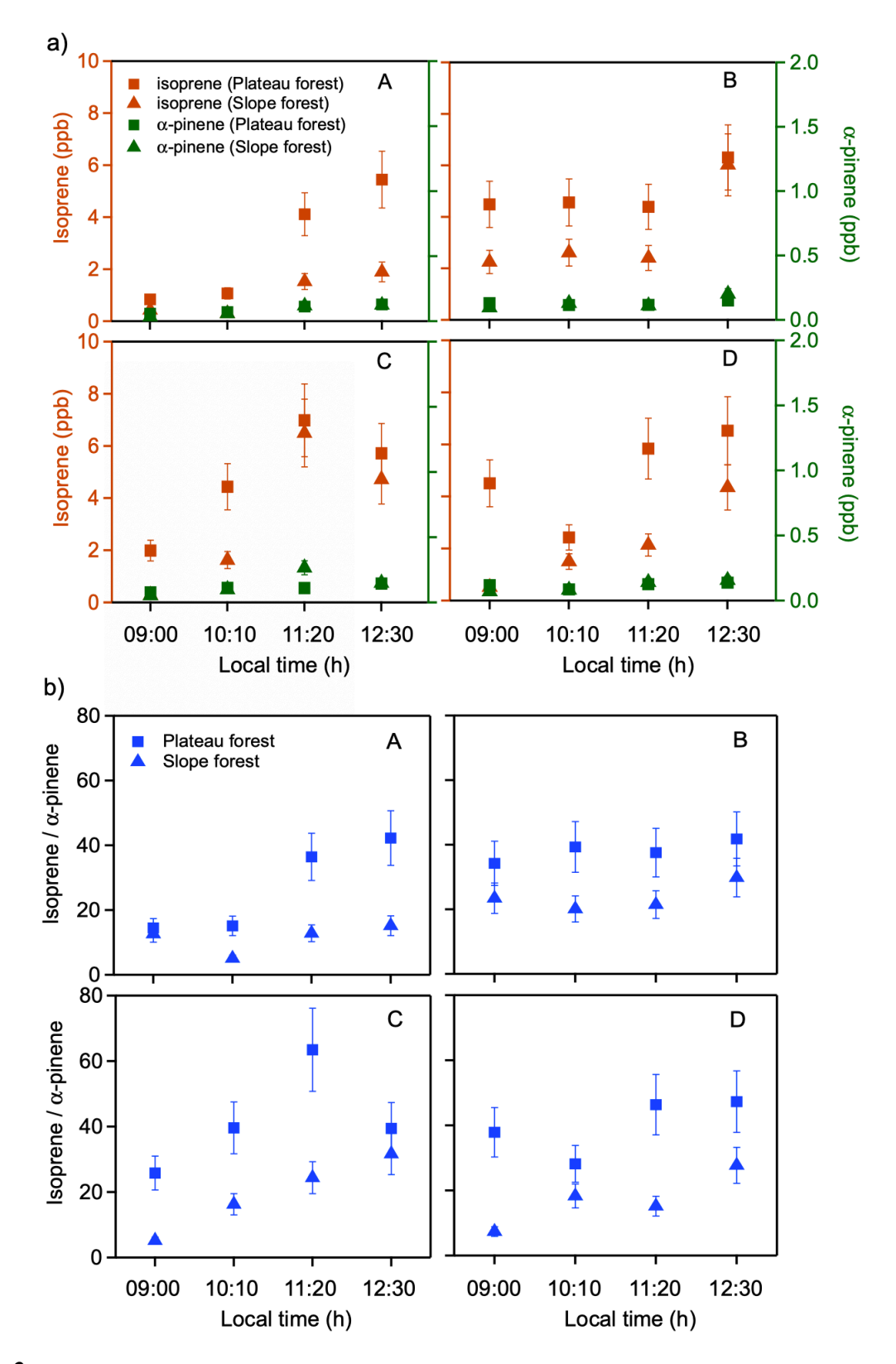


Figure 3

## **Supplementary Information**

# Intermediate-scale horizontal isoprene concentrations in the near-canopy forest atmosphere and implications for emission heterogeneity

Carla E. Batista, a,b,1 Jianhuai Ye,c,1,2 Igor O. Ribeiro, a,b Patricia C. Guimarães, a,b Adan S. S. Medeiros, a,b,d Rafael G. Barbosa, Rafael L. Oliveira, Sergio Duvoisin Jr., a,b Kolby J. Jardine, Dasa Gu,f,# Alex B. Guenther, Karena A. McKinney, Leila D. Martins, Rodrigo A. F. Souza, a,b,2 Scot T. Martin, c.i,2

<sup>a</sup>Post-graduate Program in Climate and Environment, National Institute of Amazonian Research and Amazonas State University, Manaus, Amazonas, 69060-001, Brazil

<sup>b</sup>School of Technology, Amazonas State University, Manaus, Amazonas, 69065-020, Brazil

<sup>c</sup>School of Engineering and Applied Sciences, Harvard University, Cambridge, Massachusetts, 02138, USA

<sup>d</sup>Advanced Study Center at Tefé, Amazonas State University, Tefé, Amazonas, 69553-100, Brazil

<sup>e</sup>Climate and Ecosystem Sciences Division, Lawrence Berkeley National Laboratory, Berkeley, California, 94720, USA

<sup>f</sup>Department of Earth System Science, University of California, Irvine, California, 92697, USA

gDepartment of Chemistry, Colby College, Waterville, Maine, 04901, USA

<sup>h</sup>Department of Chemistry, Federal University of Technology-Paraná, Londrina, Paraná, 86047-125, Brazil

<sup>i</sup>Department of Earth and Planetary Sciences, Harvard University, Cambridge, Massachusetts, 02138, USA

\*Now at: Division of Environment and Sustainability, Hong Kong University of Science and Technology, Hong Kong, China

<sup>1</sup>These authors contributed equally to this study.

<sup>2</sup>Correspondence to: Jianhuai Ye (jye@seas.harvard.edu), Rodrigo A. F. Souza (souzaraf@gmail.com), and Scot T. Martin (scot martin@harvard.edu)

section S1. Comparison to isoprene concentrations reported in the literature for Amazonia

Literature reports of isoprene concentrations in Amazonia are summarized in Table S4. The reported concentrations range from <1 ppb to 27 ppb. For comparison to results herein, a strong diel behavior in isoprene concentrations makes comparisons somewhat challenging. There are approximately no emissions at night, and the strongest emissions are in the early afternoon. Many literature reports are 24-h means whereas the mean values reported herein are for 09:00 to 13:30 (LT). The averaging times are listed in Table S4. In addition, some studies report mixed layer concentrations, hundreds of meters above the forest, while others describe observations near the forest where concentrations are higher. The emissions also vary strongly with season and location. Some reported concentrations also pertain to open-field locations rather than over forest canopies. The study of Yáñez-Serrano et al. (1) is most comparable to the conditions of the experiments herein. That study reports quartiles of daily isoprene concentrations at hourly resolution across a study period at a location northeast of Manaus. The upper quartile for 09:00 to 13:30 changed from 1.5 to 3.0 ppb, which is consistent to the values of 2.4 ppb and 4.4 ppb reported herein. The values observed at Ducke Reserve in this study thus appear within the range reported in the literature.

#### **section S2**. Numerical simulation

## a. Gradient transport model

The two-dimensional continuity of Equation 1 is solved by the method of lines (2-4).

$$\frac{\partial C}{\partial t} = -u \frac{\partial C}{\partial x} + K \frac{\partial^2 C}{\partial z^2} + R \tag{1}$$

This equation is called a gradient transport model in the flux literature, which is one form of a Reynolds-averaged Navier-Stokes equation (5, 6). The equation simplifies the lower part of the

atmosphere as an incompressible fluid at constant pressure and takes into consideration longitudinal advection  $(-u\frac{\partial C}{\partial x})$ , vertical convection  $(K\frac{\partial^2 C}{\partial x^2})$ , and chemistry (R). Symbols in the equation include the isoprene concentration C(x,z;t), time t, the longitudinal wind speed u, the eddy diffusion coefficient K, and the reaction rate R, all within a two-dimensional coordinate scheme of distance x and height z. Compared to the longitudinal advection (x) in the directions of the winds and the vertical convection (z) in turbulent eddies, the scale of transverse mixing (y) is small in the domain considered for the prevailing wind speeds. Therefore, this process is omitted from the model. Possible differences in local upslope and downslope transport due to forest type are taken as negligible due to insignificant differences in the Bowen ratio measured for similar forest sub-types in the wet season of central Amazonia (7).

Parameter values and data sources for use in Equation 1 are listed in Table S6. Wind speed and direction at tower height were measured. Isoprene during mid-morning hours over the tropical forest reacts dominantly with OH and O<sub>3</sub>, giving rise to the formulation of reactive chemical loss:  $R = -(k_{\rm ISOP+OH} [{\rm OH}] + k_{\rm ISOP+O3} [{\rm O_3}])$  C, in which the bimolecular rate constant  $k_{\rm ISOP+OH}$  for reactive loss of isoprene with OH and the constant  $k_{\rm ISOP+O3}$  for loss with O<sub>3</sub> are represented. The chemical lifetime  $\tau$  is given by C/R. The notation of [OH] and [O<sub>3</sub>] represents the concentrations of OH and O<sub>3</sub>, respectively. Emissions, given by  $\alpha E$  where  $\alpha$  is a relative emission factor and E is a baseline emission factor. Possible variations in all quantities of Table S5 along the course of the day in response to available sunlight are omitted from the analysis.

A set of 50 ordinary differential equations (ODEs) is constructed across altitude. The initial condition is C(x,z) = 0, corresponding to an absence of isoprene throughout the simulation domain at initial time. The upwind boundary condition corresponds to  $C(x^*,z) = 0$  where  $x^*$  is upwind limit of the simulation domain. A second boundary condition is the emission flux of

 $\alpha E(x)$  for z=0. The coupled ODEs are numerically solved by *IntegrateODE* package in Igor Pro (Version 6.38; WaveMetrics, Inc.) using the Bulirsch-Stoer algorithm for a calculation step size of 0.01 and an error scaling constant of 1.0. Simulations are carried out until a steady-state concentration at the point of UAV sampling is obtained, corresponding to  $10^4$  s in the simulation.

In respect to the computational implementation of the Equation 1,  $x^*$  is taken large enough such that  $C(x^{\dagger}, z^{\dagger})$  approaches a limiting value for long t, where  $x^{\dagger}$  and  $z^{\dagger}$  are the coordinates of UAV sampling. The maximum possible relevant domain size (i.e., for  $x^*$ ) depends on wind speed and chemical lifetime. In five lifetimes, isoprene concentration drops by more than 99%. In this case,  $x^*$  of 5  $u^{\dagger}\tau$  is appropriate. Wind speed is taken at the height ( $^{\dagger}$ ) of UAV measurement. The wind speed at altitude is estimated using a standard relationship:  $u(z) = (u^f / \kappa_V) \ln[(z-d)/z_0]$ , where  $u^f$  is the friction velocity,  $\kappa_V$  is the von Kármán constant (0.40),  $z_0$  is the roughness length (taken as 1/30 of the canopy height of 30 m), and d is the displacement height (taken as 3/4 of the canopy height h) (8). A friction velocity of 0.25 m s<sup>-1</sup> is used, which is typical for wind profiles measured in central Amazonia (Fig. S3) (9). Equation 1 assumes an absence of dry deposition for isoprene, which is typically small for tropical forests (10). The chemical lifetime  $\tau$  is calculated as  $\tau = (k_{\rm ISOP+OH} [\rm OH] + k_{\rm ISOP+O3} [\rm O_3])^{-1}$ , which assumes constant  $\tau$  throughout the simulation domain. The maximum possible relevant domain size  $x^*$  is not the footprint; rather, it is the maximum domain size that is relevant to investigation of the footprint. For the vertical coordinate, the maximum possible relevant domain size, denoted by  $z^*$ , is taken by the smaller of (i) the boundary layer height of 1000 to 1500 m of the mixed daytime atmosphere over the tropical forest or (ii) several multiples of  $\sqrt{K\tau}$  as the solution to the case of the diffusion equation for a continuous input at a fixed location followed by reactive loss (11-13).

Equation 1 represents convection by effective eddy diffusion (11). Although other approaches such as large eddy simulation can be more accurate with respect to turbulence and convection, there is a high requirement for detailed information on the parameters of the local atmospheric physics. Treatment by effective eddy diffusion can provide approximate results when less information is available to constrain local physics. The approximate results are acceptably accurate provided that the time interval of data collection exceeds one over the frequency of the largest eddies. This condition holds for the sampling method of this study, which represent collections of 2.5 min across 4 sampling days.

## b. Estimate of eddy diffusion coefficient *K*

The parameter having the most uncertain value in Equation 1 is the eddy diffusion coefficient K. Two independent methods are used to estimate the value of K, one based on Monin-Obukhov similarity theory and one based on constraints from field measurements. The two methods suggest a value of K of 30 m<sup>2</sup> s<sup>-1</sup> at the top of the canopy for the reference case of the simulation. The methods are as follows.

**Method 1.** Based on the Monin-Obukhov similarity theory (1, 14),

 $K = u^f \kappa_V (z-d)/(1-16(z-d)/L)^{-1/2}$  where  $u^f$  is the friction velocity (0.25, Fig. S3),  $\kappa_V$  is the von Kármán constant (0.40), d is the displacement height (22.5 m, taken as 3/4 of the canopy height h of 30 m), L is the Monin-Obukhov length, and -2 < (z-d)/L < 0 for daytime unstable conditions (8). The estimated K ranges from 3 to 16 m<sup>2</sup> s<sup>-1</sup> at the UAV sampling height. This method is considered biased low, however, over surfaces without non-slip conditions such as forest-atmosphere interfaces; this interface has canopy-induced wake at the boundary, introducing a roughness sublayer. Studies on turbulent structure of canopy flows suggest that the eddy diffusion coefficient in the region just above the canopy  $(h < z \le 3h)$  can increase by up to

three times (8, 15, 16), in contradistinction to the no-slip condition of smooth wall interfaces for which eddies decrease on approach to the interface. This physics suggests that the K value can range from 9 to 48 m<sup>2</sup> s<sup>-1</sup> at the top of the forest canopy.

**Method 2.** The value of K is constrained by isoprene vertical profiles measured along the height of a tower in central Amazonia. These measurements from forest canopy to 80 m constrain K from 3 to 30 m<sup>2</sup> s<sup>-1</sup> at the top of the canopy (Fig. S4).

Given the convergence of these two independent methods, for the reference case of the simulations herein a value of K of 30 m<sup>2</sup> s<sup>-1</sup> at the top of the canopy is used (Table S5).

### section S3. Zones of influence

Concentration sampled at the UAV location represents assembly contributions from the emissions of the underlying forests and the upwind forests. The analysis, therefore, focuses on four zones of influence  $x_1, x_2, x_3$ , and  $x_4$  that respectively determine 0 to 25%, 25 to 50%, 50 to 75%, and 75 to 95% of the concentration  $C^{\dagger}$  sampled at the UAV position in the atmosphere. The dagger ( $^{\dagger}$ ) symbol indicates that the concentration was calculated as  $\alpha = 1$  for all x. Values of  $x_1$ ,  $x_2, x_3$ , and  $x_4$  represent the upwind distance of each zone relative to the location of UAV sampling. Values of  $x_1, x_2, x_3$ , and  $x_4$  are obtained by (i) introducing a split boundary condition as  $\alpha = 1$  for  $x \le x'$  and  $\alpha = 0$  otherwise and (ii) carrying out stepwise increases in x' in a series of simulations to determine 0.25  $C^{\dagger}$  for  $x_1$  (i.e.,  $x_1 = x'$  when this condition holds), 0.50  $C^{\dagger}$  for  $x_2$ , 0.75  $C^{\dagger}$  for  $x_3$ , and 0.95  $C^{\dagger}$  for  $x_4$ . Uniform emissions are assumed (i.e.,  $\alpha = 1$  regardless of x), which differentiates the concept of zones of influence from the related concept of footprint (26).

Sensitivity analyses were performed to evaluate the effects of the uncertainty in model parameters on the zones of influence. The parameter having the most uncertain value in the

model is the vertical eddy diffusion coefficient K due to a lack of measurements. Increasing the eddy diffusion coefficient promotes the vertical transport of VOCs (Fig. S5). However, no significant impact on the first zone of influence  $x_1$ , meaning the nearby forest affecting the 25%level of concentrations at the point of UAV measurements, was observed (Table S5, rows 2 and 3). This result is further consistent with observations of vertical profiles of isoprene concentration reported in the literature, with which there is consistency with the simulated vertical profiles for all cases in Table S5 (Figs. S4 and S5). Additional sensitivity studies for  $x_1$ , including the effects of uncertainty in horizontal wind speed, possible horizontal heterogeneity of the Bowen ratio, and isoprene lifetime, are presented in Table S7. The main results do not change across the range of considered uncertainties. For a central value of 150 m,  $x_1$  varies from 100 to 250 m across the sensitivity analysis. Finally, strong coherent eddies can sometimes develop at the canopy edge (15, 17-19), and these coherent eddies sweep into the forest, promoting the exchange of air between the forest and the overlaying atmosphere and leading to strong ejections (i.e., increase K near the canopy surface). These sweep-ejection cycles extend to the whole canopy on the time scale of minutes (20, 21). Without quantitative information, the effects of this mechanism were investigated herein by supposing 20% dilution of isoprene concentration in the near-canopy air every 1 min. This mechanism, if active, further decreases  $x_1$ to 100 m (row 4, Table S5).

An important aspect of the model treatment is the level of OH concentration that represents the degree the role of pollution in the area because the UAV sampling was conducted on the northern outskirts of Manaus. The OH concentration in the reference case is representative of the chemistry of polluted conditions in central Amazonia (22). Given that OH concentration was not measured in the present study, a sensitivity test was carried out by decreasing the OH

concentration by a factor of 3 to represent background regional conditions (14, 23). The value of  $x_1$  became 500 m (row 5, Table S5). Further results are plotted in Fig. S5.

# section S4. Unmanned aerial vehicle and VOC sampler

The UAV was a DJI Matrice 600 Professional Grade. It was a hexacopter design with onboard stabilization. The maximum ascent rate was 5 m s<sup>-1</sup>, and the maximum horizontal speed was 18 m s<sup>-1</sup>. It had GPS positioning and maintained two-way communication with DJI control programs deployed on a tablet computer (mini-iPad, Apple Inc.). The UAV had a nominal flight time of 30 min. The VOC sampler was mounted to the flight platform. Testing for the sampler mass indicated 25 min of flight time, including a margin of security of an additional 5 min. Actual battery use in each flight depended on the flight plan and the strength of local winds during the flight.

The sampler mounted to the UAV was described in Ref. (24). In brief, samples were collected by drawing air through cartridge tubes packed with Tenax TA and Carbograph 5TD (C2-AXXX-5149, Markes International, Inc.; outer diameter of 6.35 mm; length of 9 cm). The sorbent materials were hydrophobic and suitable for air sampling at high relative humidity (25). A sample flow rate of 0.15 L min<sup>-1</sup> was used for collection. After sampling, the cartridge tubes were removed from the UAV sampler, capped using Swagelok fittings outfitted with Teflon ferrules (PTFE), and stored at room temperature prior to shipping to Irvine, California, USA, where they were stored in a refrigerator prior to chromatographic analysis. Additional samples were collected directly from the tower platform at Location A using a handheld pump (GilAir PLUS, Gilian) to draw air through cartridge tubes, after which they were also capped and stored in the same manner.

## **section S5.** Chemical analysis

Thermal desorption gas chromatography was used to analyze the samples. The cartridge tubes were loaded into a thermally desorbing autosampler (TD-100, Markes International, Inc) and heated to 285 °C for 6 min with helium carrier gas. The desorbed VOC were cryofocused at -10 °C on a cold trap and then heated to 290 °C to release the VOC. A flow of 6.2 mL min<sup>-1</sup> was split so that 19% was transferred to the column (30 m, DB-5) of a gas chromatograph (GC, model 7890B, Agilent Technologies, Inc). A multi-step temperature ramp was used from -30 °C to 260 °C. Detectors included a time-of-flight mass spectrometer (Markes BenchTOF-SeV) and a flame ionization detector (TD-GC-FID/TOFMS). The compounds were identified by mass spectra and retention time and quantified by FID using authentic standards (26).

The responses to isoprene and  $\alpha$ -pinene concentrations, which are the focus of the data presentation herein, were calibrated by loading known amounts into cartridge tubes followed by analysis with the same protocols as used for the atmospheric samples. The analytical system had a detection limit of 1 pg for isoprene and  $\alpha$ -pinene. The overall detection limit for the atmospheric samples, however, was higher than the limit of the analytical system because the background levels for cartridge tubes exposed to air (i.e., blanks) in the absence of drawn flow for the corresponding time period (i.e., samples) had a typical mass loading of 10 pg. These results corresponded to an approximate uncertainty in the analytical method of 2 ppt for a 3-L sample. The precision was 5% ( $\alpha$ -pinene) to 10% (isoprene). The total uncertainty was 2 ppt or 10%, whichever was greater. An additional uncertainty of 15% was related to the measured flow of the VOC sampler. The overall combined measurement uncertainty was estimated as 20%, as discussed further in Ref. (24).

**Table S1.** Plant families and species of the valley, slope, and plateau regions of the Ducke Reserve. Source: Ribeiro et al. (27).

	Valley Forest		Slope Forest		Plateau Forest
Plant Family	Species	Plant Family	Species	Plant Family	Species
Arecaceae	Oenocarpus bataua Mart.	Arecaceae	Oenocarpus bacaba Mart.	Arecaceae	Attalea attaleoides (Barb. Rodr.) W. Boer
	Socratea exorrhiza (Mart.) H.A. Wendl.		Astrocaryum sciophilum (Miq.) Pulle		
	Mauritia flexuosa L. f.				
	Attalea spectabilis Mart.				
Clusiaceae	Symphonia globulifera L.				
				Caryocaraceae	Caryocar villosum (Aublet) Pers.
					Caryocar glabrum (Aublet) Pers.
Fabaceae	Hymenolobium sp.	Fabaceae	Dinizia excelsa Ducke	Fabaceae	Dinizia excelsa Ducke
					Dipteryx odorata (Aublet) Willd.
Lecythidaceae	Allantoma lineata (Mart. ex Berg) Miers	Lecythidaceae	Eschweilera sp.	Lecythidaceae	Cariniana micrantha Ducke
					Eschweilera sp.
Meliaceae	Carapa guianensis Aublet			Mimosaceae	Marmaroxylon racemosum (Ducke) Killip
Rapataceae	Rapatea paludosa Aublet				
Sapotaceae	Pouteria sp.				
	Chrysophyllum sanguinolentum (Pierre) Baehni				
				Solanaceae	Duckeodendron cestroides kuhlm.

**Table S2.** Isoprene and  $\alpha$ -pinene concentrations, start times for sample collection, and atmospheric state variables. "Local time (LT) measurements (i.e., cartridge tube "1"). <sup>d</sup>Uncertainty in concentrations is 20%. See main text. period. For example, the first row represents the mean concentration from 09:00 to 10:00 (LT) across the week of not contribute to the reported weekly mean. Entries in the first four rows of each week represent weekly means at that time tube each hour. Entries marked by "-" indicate that no sampling was carried out in this flight, meaning that this flight did cartridge tube. The sampling duration was 2.5 min for each flight, corresponding to 5 min of collection in each cartridge was 4 h earlier than UTC. bTwo flights ("Flight 1" and "Flight 2") of 25 min per flight took place each hour with the same

	23Feb18				22Feb18				21Feb18			Date	Data
2	1	4	3	2	1	4	ယ	2	3 1		Identifier	Cartridge Tube	
10:04	ı	12:04	11:04	ı	09:04	ı	11:09	ı	-		$\begin{array}{c} {\sf Time} \\ ({\sf LT})^{a,b} \end{array}$	Start	T::~L4 1
10:34	ı	12:34	11:34	10:34	ı	12:49	11:39	ı	-		Time (LT)	Start	T1:~L+ 3
						5.45	4.12	1.07	0.84		$\begin{array}{c} \text{(ppbv)} \\ \text{Location A}^{c,d} \end{array}$	Isoprene	Washir Mass
						1.90	1.53	0.30	0.43	Week 1	(ppbv) Location B	Isoprene Isoprene	Washir Mass
						0.13	0.11	0.07	0.06		(ppbv) Location A	weekiy Mean α-pinene	
						0.13	0.12	0.06	0.03		(ppbv) Location B	weekly меан Almospheric Lemp Kel a-pinene State (°C) Hum	Washir Mass
sunny		cloudy	cloudy	cloudy	cloudy	cloudy	cloudy	ı	'			Atmospheri State	A tanaan haui
26.3 89.4	25.4 92.0	27.7 82.3	27.2 85.2	26.2 89.8	25.2 94.2	29.4 69.2	28.8 72.9	28.2 77.2	27.4 82.4		(%)	(°C) Hum	Tama Dal

02Mar18		01Mar18	28Feb18		27Feb18	24Feb18
6 5	8 7 6	5 & 7	6	2 2	1 4 3 2	1 4 3
09:04	11:04	11:04 12:04	09:04	10:04	10:04 11:04 12:04 09:04	11:04 - 09:04
09:34	10:34 11:34	11:34 12:34 -	09:34 10:34	10:34	10:34 11:34 12:34 09:34	- 09:34
		4.39 6.31	4.49 4.56			
		2.41 6.02	Week 2 2.25 2.61			
		0.12 0.15	0.13 0.12			
		0.11 0.20	0.10			
strong wind clear, sunny, 28.2 78.6 wind clear, sunny, 29.9 70.7 wind	clear, sunny, strong wind clear, sunny, strong wind		clear, sunny	rainy cloudy and rainy -	cloudy cloudy cloudy cloudy	sunny - cloudy
28.2	29.7 30.4	27.4 28.8 27.9	25.6 92.3 26.6 87.7	25.0 92.3 25.0 93.0 24.4 92.7	24.7 93.4 25.3 92.0 26.8 85.0 25.0 92.5	27.5 27.7 24.1
78.6	76.3 72.2	85.7 80.2 82.0	92.3 87.7	92.3 93.0 92.7	93.4 92.0 85.0 92.5	85.0 83.2 94.5

89.3	27.5	sunny, strong 27.5 89.3 wind					10:03	09:32	9	07Mar18
93.4	25.9 93.4	ı	0.15	0.15	4.72	5.72	ı		12	
92.4	26.4 92.4	1	0.27	0.11	6.50	6.98			11	
83.7	28.5	cloudy, wind 28.5	0.10	0.11	1.63	4.44	10:57	10:28	10	
84.9	28.4	cloudy, wind 28.4 84.9	0.05	0.08	0.28	1.99	09:55	09:25	9	06Mar18
					Week 3					
		cloudy, rain around								
85.4	28.8 85.4						12:34	12:04	∞	
		cloudy, rain								
86.8	28.3						11:34	11:04	7	
		around								
		cloudy, rain								
93.0	27.5 93.0						10:34	10:04	6	
		around								
		in.								
92.2	26.9 92.2	partly					09:34	09:04	5	05Mar18
74.8	29.8						1	,	∞	
		cloudy								
74.8	29.8 74.8						ı	11:04	7	
		cloudy								
76.5	30.0 76.5						10:34	10:04	6	
		cloudy								
86.0	28.6 86.0						09:34	09:04	2	03Mar18
		wind								
60.8	32.1	clear, sunny, 32.1 60.8					12:34	12:04	∞	
		wind								
64.4	31.2	clear, sunny, 31.2 64.4					ı	11:04	7	

27.9 80.8	27.9	•	0.16	0.14	4.35	6.53	ı	,	16	
75.6	28.7	partly cloudy 28.7 75.6	0.14	0.13	2.14	5.84	ı	12:07	15	
76.8	28.6	partly cloudy 28.6 76.8	0.08	0.09	1.50	2.43	11:13	10:42	14	
80.7	28.0	partly cloudy 28.0	0.07	0.12	0.52	4.51	10:08	09:41	13	12Mar18
					Week 4					
		strong wind								
82.7	28.2						12:26	12:03	12	
		strong wind								
86.2	27.7	cloudy, very					10:18	10:46	11	
		strong wind								
91.5	26.4 91.5	,					10:15	09:45	10	
95.7	25.3 95.7	cloudy, very					09:13		9	10Mar18
. 94.9	24.4	ı					ı	1	12	
80.8	28.4	ı					•		11	
		strong wind								
84.0	28.9 84.0						10:32	10:03	10	
89.	27.7	cloudy,					10:01	09:00	9	09Mar18
81.:	29.2 81.5	cloudy					13:10	12:42	12	
83.7	28.6						12:10	ı	11	
88.2	27.4						11:02	ı	10	
91.2	26.5	cloudy					09:57	09:26	9	08Mar18
		wind								
76.4	29.9	sunny, strong 29.9 76.4					13:21	12:50	12	
		strong wind								
82.0	28.5						12:09	11:38	11	
		strong wind								
84.(	28.4 84.0	cloudy,					11:06	10:34	10	

.7 88.3	partly cloudy 26.7	12:59	2:17	16	
7.7 84.4	partly cloudy 27.7	11:44	1:14		
.5 85.8	partly cloudy 27.5	10:34	ı		
0 91.6	partly cloudy 26.0	10:04	1		27Mar18
.3 84.7	cloudy 28.3	13:25	2:50	16	
9 90.7	cloudy 26.9	12:20	ı		
.2 91.7		10:59	0:28		
2 96.4	cloudy 26.2	09:59	9:29		15Mar18
	partly cloudy 29.3	13:22	2:49		
.5 80.4	partly cloudy 28.5	12:14	1:49		
	partly cloudy 27.2	11:19	0:48		
6.6 91.7	partly cloudy 25.6	10:18	09:49		14Mar18
.4 92.7	- 26.4	•	1	16	
.0 96.8	cloudy 25.0	12:07	1:34		
.2 98.9	- 24.2	1	ı	14	
.7 99.7	- 23.7	•	ı	13	13Mar18

**Table S3.** Calculated probability (p-value) for the null hypothesis that two sets of concentrations are the same over location A and location B for the full campaign (weeks 1 - 4; N = 16) and individual weeks (N = 4), where N is the number of points included in each analysis. Results are shown for isoprene and α-pinene.

Time	Isoprene	α-pinene
Weeks 1 through 4	<0.001	0.61
Week 1	0.09	0.26
Week 2	0.04	0.75
Week 3	0.06	0.51
Week 4	0.03	0.78

**Table S4.** Isoprene concentrations measured in different regions of Amazonia. "Sampling at most tower sites was 10 to 20 m above and Alves et al. (29). earlier than UTC. <sup>c</sup>Wet-to-dry transition season (WDT) and dry-to-wet transition season (DWT). Sources: Harley et al. (28) the top of the forest canopy. The sampling at the ATTO tower was up to 50 m above the canopy. <sup>b</sup>Local time (LT) was 4 h

÷		Latitude /	Land	Isoprene	Averaging	$\mathbf{Height}^a$	
Location	Season	longitude	topography	(ppb)	time	ð	Study
Adolfo Ducke Forest	Wet	3.0032° S, 59.9397° W	Plateau	4.4	$09:00-13:30 \ (LT)^b$	Ducke - tower	this study
Reserve (Amazonas, Brazil)	Wet	2.9988° S, 59.9364° W	Slope	2.4	09:00-13:30 (LT)	Ducke - tower	this study
Nossa Senhora Aparecida Farm (Rondônia, Brazil)	Wet	10.7667° S, 61.3333° W	Plateau	1.5	ı	Balloon	Ref. (30)
Jaru Biological Reserve (Rondônia, Brazil)	Wet	10.1333° S, 61.9000° W	Plateau	6.7	1	Balloon	Ref. (30)
GoAmazon2014/5 T3 Site	Dry	3.2133° S, 60.5987° W	Open Field	6	ı	Aircraft (500 m)	Ref. (31)
(Amazonas, Brazil)	Wet	3.2133° S, 60.5987° W	Open Field	5	ı	Aircraft (500 m)	Ref. (31)
Tapajós National Forest	Wet	2.8500° S, 54.9667° W	Plateau	0.5	ı	Balloon	Ref. (30)
(Pará, Brazil)	$\mathrm{WDT}^c$	2.5100° S, 54.5800° W	Plateau	5	06:00-18:00 (LT)	Low tower	Ref. (32)

**Table S5.** Sensitivity analysis for different models of near-surface mixing. For each case, the distances  $x_1$ ,  $x_2$ ,  $x_3$ , and  $x_4$  for the zones of influence are listed. \*Table S6 presents values used in the reference case. \*\*Gradient from 30 to 10 m<sup>2</sup> s<sup>-1</sup> from canopy to 3*h* and 10 m<sup>2</sup> s<sup>-1</sup> for >3*h*. Canopy height *h* varied from 25 to 35 m at the sampling locations. \*\*\*Noontime hydroxyl radical concentration of  $2.0 \times 10^{12}$  molec m<sup>-3</sup> for background conditions (14, 23).

				Zo	nes o	f Influ	ence
Physical or chemical	Eddy	VOC	Lifetime $ au$	$x_1$	$x_2$	<i>x</i> <sub>3</sub>	<i>x</i> <sub>4</sub>
processes	diffusion	species	against	(m)	(m)	(m)	(m)
	coefficient		reactive loss				
	$K (m^2 s^{-1})$		<b>(s)</b>				
Reference case*	30 to 10 m <sup>2</sup> s <sup>-1</sup> ;	isoprene	1630	150	700	2350	8300
(Polluted)	$10 \text{ m}^2 \text{ s}^{-1**}$						
Polluted	15 to 5 m <sup>2</sup> s <sup>-1</sup> ;	isoprene	1630	150	650	2250	7750
	$5 \text{ m}^2 \text{ s}^{-1}$						
Polluted	300 to 100 m <sup>2</sup>	as above	as above	150	950	3300	11850
	s <sup>-1</sup> ; 100 m <sup>2</sup> s <sup>-1</sup>						
Polluted + Sweep-	30 to 10 m <sup>2</sup> s <sup>-1</sup> ;	as above	as above	100	450	1550	6350
Ejection (20% dilution)	$10 \text{ m}^2 \text{ s}^{-1}$						
Background regional	as above	as above	4900	500	2950	10350	33400
conditions***							

**Table S6.** Parameter values for Equation 1. Values in parentheses are used in the reference case of the simulation. \*The comparative lifetime of  $\alpha$ -pinene is 2510 s.

Quantity	Symbol	Value	Units	Source
Bimolecular rate constant of isoprene with hydroxyl radical	k <sub>ISOP+OH</sub>	1 × 10 <sup>-16</sup>	molec m <sup>-3</sup> s <sup>-1</sup>	Ref. (36)
Bimolecular rate constant of isoprene with ozone	k <sub>ISOP+O3</sub>	$1.3 \times 10^{-23}$	molec m <sup>-3</sup> s <sup>-1</sup>	Ref. (36)
Hydroxyl radical concentration	[OH]	$0.2 \text{ to } 9 (6.0) \times 10^{12}$	molec m <sup>-3</sup>	Refs. (14, 23, 31)
Ozone concentration	$[O_3]$	2.5 to 5.0 (10.0) $\times$ 10 <sup>17</sup>	molec m <sup>-3</sup>	Ref. (31)
Isoprene lifetime against chemical loss	τ	1630*	S	$(k_{\text{ISOP+OH}} [\text{OH}] + k_{\text{ISOP+O3}} [\text{O}_3])^{-1};$ $R = C / \tau$
Horizontal wind speed (advection)	u	1 to 3 (1.8)	m s <sup>-1</sup>	Measured in late morning hours at top of tower (Fig. S1)
		2 to 4 (2.5)	m s <sup>-1</sup>	Estimated at 50 m above canopy. See section S2.
Eddy diffusion coefficient (at canopy top)	K	3 to 30; 9 to 48; 300 (30)	$\mathrm{m^2~s^{\text{-}1}}$	See section S2.

**Table S7.** Sensitivity analysis for the first zone of influence  $x_1$  to parameter values used in Equation 1 for the reference case of the model (Table S5). \*The eddy diffusion coefficient at the UAV sampling site  $(x = x^{\dagger})$  was treated as  $2 \times$  or  $0.5 \times$  of those of the upwind forest  $(x < x^{\dagger})$  to examine the effect of the heterogeneity of Bowen ratio over different forest sub-types. \*\*The distances associated with  $x_3$  and  $x_4$  might be sufficiently upwind of the urban region such that the OH concentration remains at the background concentration; the sensitivity test represented in the final row of the table uses an OH concentration representative of polluted conditions for 0 to 5000 m (i.e., as for the reference case) and an OH concentration representative of background conditions beyond 5000 m (i.e., 3 times lower than polluted conditions).

Quantity	Change (9/)	y (m)	Change in x <sub>1</sub>
Quantity	Change (%)	$x_1$ (m)	(%)
Reference case (Tables S5 and S6)	n/a	150	n/a
u	+25%	200	+33
	-25%	100	-33
τ	+25%	100	-33
	-25%	200	+33
$K^*$	$K_{x=x^{\dagger}} = 2K_{x < x^{\dagger}}$	250	+67
	$K_{x=x^{\dagger}} = 0.5K_{x < x^{\dagger}}$	100	+33
$\tau(x)^{**}$ (background)	see caption	250	+67

**Table S8.** Isoprene concentrations sampled by the UAV platform at different heights over the plateau forest in Duke Reserve. \*Ratio of isoprene concentration at a lower sampling height over the local forest canopy (either 15 or 25 m) to that at a higher sampling height (65 m).

	Sampling	Sampling	Sampling height	Sampling height	Isoprene	
	date	time (LT)	(m, above local	(m, above local	(ppb)	Ratio*
			ground)	canopy)		
1	20170802	15:30	60	25	1.64	1.45
			100	65	1.13	
2	20170830	10:00	60	25	5.08	0.85
			100	65	5.94	
3	20170929	14:30	50	15	1.74	1.43
			100	65	1.22	
4	20171122	13:00	50	15	4.93	1.16
			100	65	4.25	
					Average	1.22

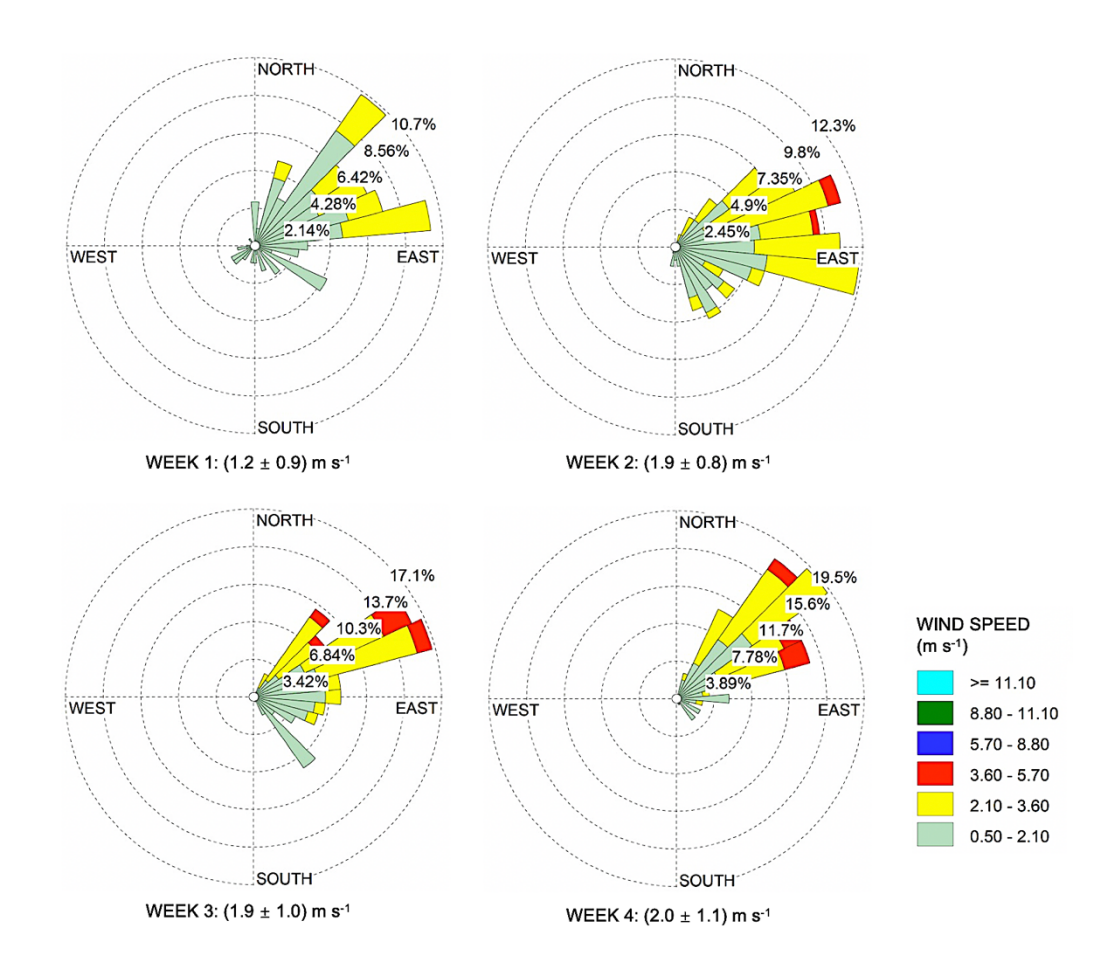


**Fig. S1.** Wind direction and speed measured by a weather station during late morning and early afternoon (09:00 to 13:30) at location A for each week of the campaign. Local time is UTC minus 4 h.

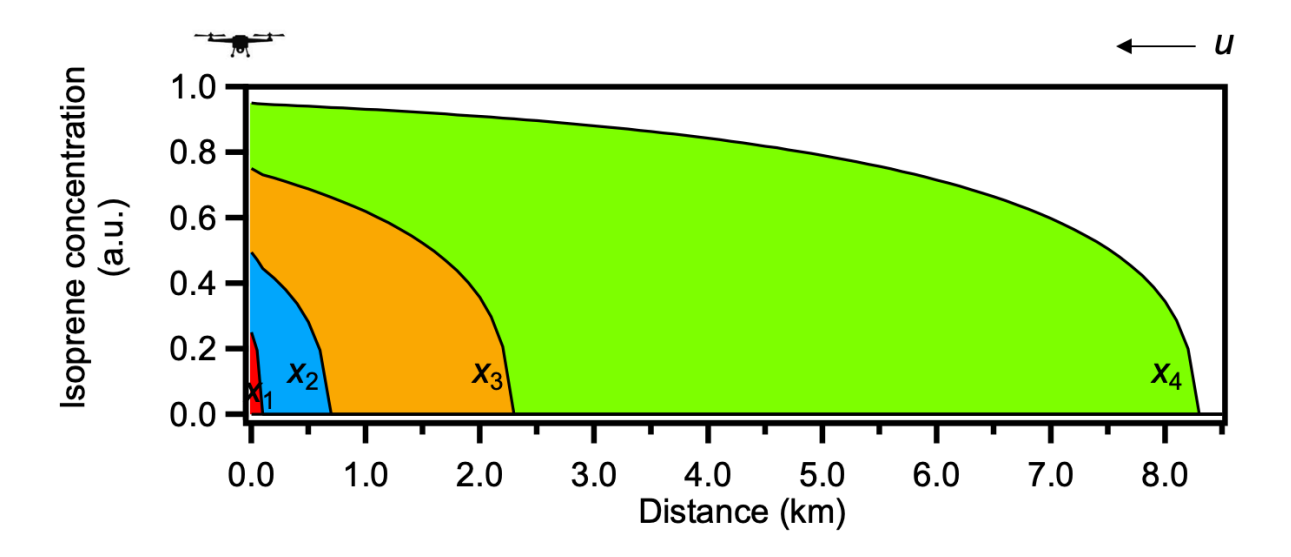
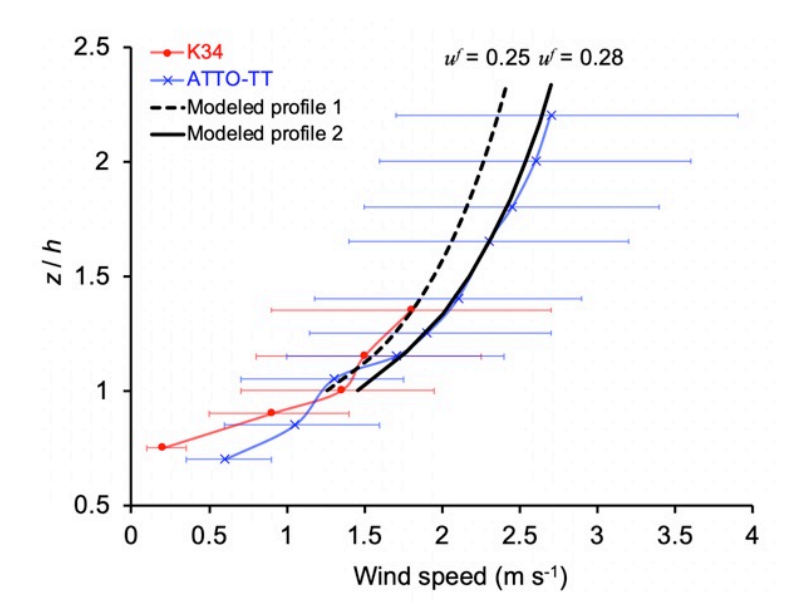


Fig. S2. Role of upwind distance of forest emissions on isoprene concentration at the location of near-canopy atmospheric sampling. Results are shown for the reference case of the model (Table S5). The ordinate at x = 0 (i.e.,  $x^{\dagger}$  and  $z^{\dagger}$  of UAV sampling) represents the fractional contribution to isoprene concentration of upwind forest emissions for the progressive distance intervals of  $x_1, x_2, x_3$ , and  $x_4$ . Zones of influence  $x_1, x_2, x_3$ , and  $x_4$  that affect the fractional concentration are colored in red, blue, brown, and green, respectively (i.e., as for the right panel of Fig. 1). The forests associated with each of the four zones are located upwind of the sampling location by 0 to 150 m ( $x_1$ ), 150 to 700 m ( $x_2$ ), 700 to 2350 m ( $x_3$ ), and 8300 m and beyond ( $x_4$ ). Uniform emissions are assumed. Isoprene concentration is normalized to the maximum concentration. "a.u." is denoted as arbitrary unit.



**Fig. S3.** Measured and modeled wind profiles. Measured profiles (mean  $\pm$  standard deviation) are adapted from Santana et al. (9) for two sites in central Amazonia (K34 and ATTO). Modeled wind profiles are estimated based on the equation presented in section S2. The ordinate quantity z/h is altitude z normalized by canopy height h.

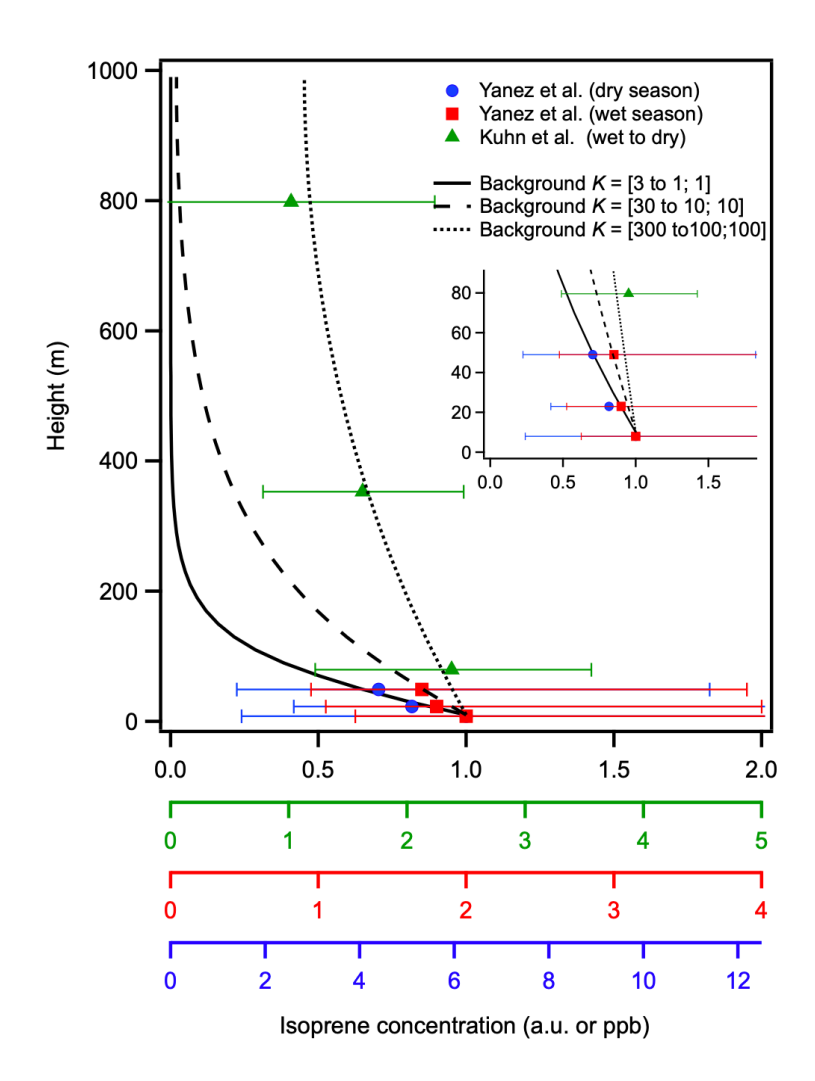
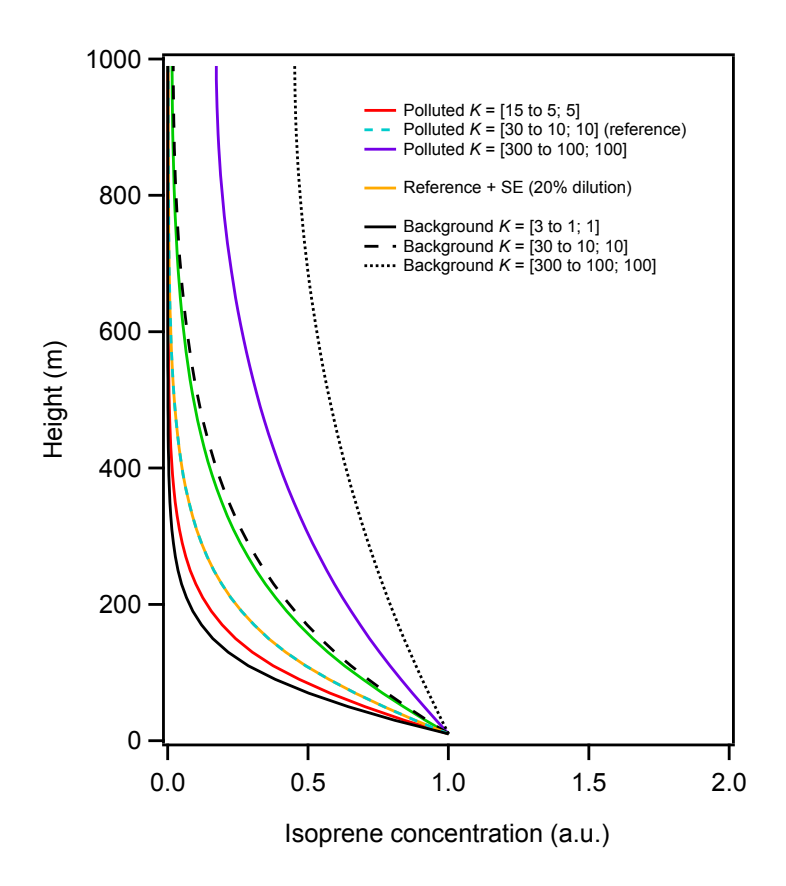


Fig. S4. Simulated vertical profiles of isoprene concentration at the point of UAV sampling for different values of the eddy diffusion coefficient K. In each simulation, a gradient of K was applied from the canopy to 3h. The K value was constant above 3h. For example, K = [3 to 1; 1] is read as a gradient of K from 3 to 1 m<sup>2</sup> s<sup>-1</sup> from canopy to 3h and 1 m<sup>2</sup> s<sup>-1</sup> for > 3h. A value for [OH] of  $2.0 \times 10^{12}$  molec m<sup>-3</sup> was used to compare the simulated profiles to observations by Yáñez-Serrano et al. (1) and Kuhn et al. (14) taken for central Amazonia under background conditions away from pollution sources of Manaus. For the simulated profiles, the isoprene concentration is represented in arbitrary units (a.u.) to remove the effects of uncertain emissions.



**Fig. S5.** Simulated vertical profiles of isoprene concentration at the point of UAV sampling for the different physical and chemical processes of Table S5. The abbreviation "SE" denotes the "sweep-ejection mechanism".

## References

- Yáñez-Serrano AM, et al. (2015) Diel and seasonal changes of biogenic volatile organic compounds within and above an Amazonian rainforest. Atmos. Chem. Phys. 15(6):3359-3378.
- 2. Jacobson MZ (2005) *Fundamentals of atmospheric modeling* (Cambridge University Press).
- 3. Mazumder S (2015) Numerical methods for partial differential equations: finite difference and finite volume methods (Academic Press).
- 4. Schiesser WE (2012) The numerical method of lines: integration of partial differential equations (Elsevier).
- 5. Alfonsi G (2009) Reynolds-averaged navier–stokes equations for turbulence modeling. *Appl. Mech. Rev.* 62(4):040802.
- 6. Lenschow D (1995) Micrometeorological techniques for measuring biosphereatmosphere trace gas exchange. *Biogenic Trace Gases: Measuring Emissions from Soil* and Water:126-163.
- 7. Broedel E, et al. (2017) Simulation of Surface Fluxes in Two Distinct Environments along a Topographic Gradient in a Central Amazonian Forest using the INtegrated LAND Surface Model. *Hydrol. Earth Syst. Sci. Discuss.* 2017:1-49.
- 8. Kaimal JC & Finnigan JJ (1994) *Atmospheric boundary layer flows: their structure and measurement* (Oxford University Press).
- 9. Santana RASd, Dias-Júnior CQ, Vale RSd, Tóta J, & Fitzjarrald DR (2017) Observing and Modeling the Vertical Wind Profile at Multiple Sites in and above the Amazon Rain Forest Canopy. *Adv. Meteorol.* 2017(5436157).

- 10. Karl T, *et al.* (2004) Exchange processes of volatile organic compounds above a tropical rain forest: Implications for modeling tropospheric chemistry above dense vegetation. *J. Geophys. Res.* 109(D18):D18306.
- 11. Bird RB (2002) Transport phenomena. Appl. Mech. Rev. 55(1):R1-R4.
- 12. Cussler EL (2009) *Diffusion: mass transfer in fluid systems* (Cambridge University Press).
- 13. Fisch G, et al. (2004) The convective boundary layer over pasture and forest in Amazonia. *Theor. Appl. Climatol.* 78(1-3):47-59.
- 14. Kuhn U, et al. (2007) Isoprene and monoterpene fluxes from Central Amazonian rainforest inferred from tower-based and airborne measurements, and implications on the atmospheric chemistry and the local carbon budget. Atmos. Chem. Phys. 7(11):2855-2879.
- 15. Finnigan J (2000) Turbulence in plant canopies. *Annu. Rev. Fluid Mech.* 32(1):519-571.
- Raupach MR, Finnigan J, & Brunet Y (1996) Coherent eddies and turbulence in vegetation canopies: the mixing-layer analogy. *Bound. Layer Meteorol.*, (Springer), Vol 25th Anniversary Volume, pp 351-382.
- 17. Fuentes JD, *et al.* (2016) Linking meteorology, turbulence, and air chemistry in the Amazon rain forest. *Bull. Am. Meteorol. Soc.* 97(12):2329-2342.
- 18. Raupach M & Thom AS (1981) Turbulence in and above plant canopies. *Ann. Rev. Fluid Mech.* 13(1):97-129.
- 19. Raupach MR & Shaw R (1982) Averaging procedures for flow within vegetation canopies. *Bound. Layer Meteorol.* 22(1):79-90.

- 20. Katul G, Porporato A, Cava D, & Siqueira M (2006) An analysis of intermittency, scaling, and surface renewal in atmospheric surface layer turbulence. *Physica D:*Nonlinear Phenomena 215(2):117-126.
- 21. Robinson SK (1991) Coherent motions in the turbulent boundary layer. *Ann. Rev. Fluid Mech.* 23(1):601-639.
- 22. Martin S, *et al.* (2017) The Green Ocean Amazon experiment (GoAmazon2014/5) observes pollution affecting gases, aerosols, clouds, and rainfall over the rain forest. *Bull. Am. Meteorol. Soc.* 98(5):981-997.
- 23. Karl T, *et al.* (2007) The tropical forest and fire emissions experiment: emission, chemistry, and transport of biogenic volatile organic compounds in the lower atmosphere over Amazonia. *J. Geophys. Res.* 112(D18):D18302.
- 24. McKinney KA, *et al.* (2019) A sampler for atmospheric volatile organic compounds by copter unmanned aerial vehicles. *Atmos. Meas. Tech.* 12: 3123-3135.
- 25. Brown VM, Crump DR, Plant NT, & Pengelly I (2014) Evaluation of the stability of a mixture of volatile organic compounds on sorbents for the determination of emissions from indoor materials and products using thermal desorption/gas chromatography/mass spectrometry. *J. Chromatogr. A* 1350:1-9.
- 26. Faiola C, Erickson M, Fricaud V, Jobson B, & VanReken T (2012) Quantification of biogenic volatile organic compounds with a flame ionization detector using the effective carbon number concept. *Atmos. Meas. Tech.* 5(8):1911-1923.
- 27. Ribeiro JELS, Nelson BW, Silva MFd, Martins LSS, & Hopkins M (1994) Reserva florestal ducke: diversidade e composição da flora vascular. *Acta Amaz.* 24(1-2):19-30.

- 28. Harley P, et al. (2004) Variation in potential for isoprene emissions among Neotropical forest sites. Glob. Change Biol. 10(5):630-650.
- 29. Alves EG, *et al.* (2016) Seasonality of isoprenoid emissions from a primary rainforest in central Amazonia. *Atmos. Chem. Phys.* 16(6):3903-3925.
- 30. Greenberg JP, *et al.* (2004) Biogenic VOC emissions from forested Amazonian landscapes. *Glob. Change Biol.* 10(5):651-662.
- 31. Liu Y, *et al.* (2018) Isoprene photo-oxidation products quantify the effect of pollution on hydroxyl radicals over Amazonia. *Sci. Adv.* 4(4):eaar2547.
- 32. Rinne H, Guenther A, Greenberg J, & Harley P (2002) Isoprene and monoterpene fluxes measured above Amazonian rainforest and their dependence on light and temperature.

  \*\*Atmos. Environ. 36(14):2421-2426.
- 33. Rizzo LV, Artaxo P, Karl T, Guenther AB, & Greenberg J (2010) Aerosol properties, incanopy gradients, turbulent fluxes and VOC concentrations at a pristine forest site in Amazonia. *Atmos. Environ.* 44(4):503-511.
- 34. Jardine KJ, *et al.* (2016) Methanol and isoprene emissions from the fast growing tropical pioneer species Vismia guianensis (Aubl.) Pers. (Hypericaceae) in the central Amazon forest. *Atmos. Chem. Phys.* 16(10):6441-6452.
- 35. Kesselmeier J, *et al.* (2000) Atmospheric volatile organic compounds (VOC) at a remote tropical forest site in central Amazonia. *Atmos. Environ.* 34(24):4063-4072.
- 36. Atkinson R & Arey J (2003) Atmospheric degradation of volatile organic compounds. *Chem. Rev.* 103(12):4605-4638.